Evaluation of the clinical utility of maximum intensity projections of 3D contrast-enhanced, T1-weighted imaging for the detection of brain metastases

Hainc, Nicolin ; Federau, Christian ; Tyndall, Anthony ; Mittermeier, Andreas ; Bink, Andrea ; Stippich, Christoph ; Schubert, Tilman

Abstract: BACKGROUND To visualize and assess brain metastases on magnetic resonance imaging, radiologists face an ever-increasing pressure to perform faster and more efficiently. The usage of maximum intensity projections (MIPs) of contrast-enhanced T1-weighed (T1ce) magnetization-prepared rapid acquisition with gradient echo (MP-RAGE) images proposes to increase reading efficiency by increasing lesion conspicuity while reducing in the number of images to be reviewed. AIM To assess if MIPs save reading time and achieve the same level of diagnostic accuracy as standard 1 mm T1ce images for the detection of brain metastases. METHODS Forty-four patients were included in this retrospective study. Axial reformations of T1ce MP-RAGE (TR/TE = 2300/2.25 ms, resolution = 1 mm^3) images were analyzed and post-processed into 5 and 10 mm MIPs. Two readers evaluated the randomly assorted images and recorded reading time. Reading time differences were analyzed using the Wilcoxon test, and inter-reader statistics were performed using Bland-Altman plots. RESULTS About 22.5 61.2 s/study and 43.8 ± 159.9 s/study were saved using 5 and 10 mm MIPs, respectively. Combined average sensitivity was 92.0% for 5 mm MIPs and 86.3% for 10 mm MIPs compared to standard 1 mm axial slices, with an average rate of 0.98 and 0.57 false positives per study, respectively CONCLUSION: While 5 mm and 10 mm T1ce MP-RAGE MIPs showed a clinical benefit in reducing reading times for evaluation of brain metastases, they should be used in conjunction with standard 1 mm images for best sensitivity and specificity, a practice which possibly annuls their benefit.

DOI: https://doi.org/10.1002/cnr2.1277

Evaluation of the Clinical Utility of Maximum Intensity Projections of 3D Contrast-Enhanced, T1-weighted Imaging for the Detection of Brain metastases.

Abstract (244 words)

Background

To visualize and assess brain metastases on MRI, radiologists face an ever-increasing pressure to perform faster and more efficiently. The usage of maximum intensity projections (MIPs) of contrast enhanced T1 weighed (T1ce) Magnetization-Prepared Rapid Acquisition with Gradient Echo (MP-RAGE) images proposes to increase reading efficiency by increasing lesion conspicuity while reducing in the number of images to be reviewed.

Aim

To assess if MIPs save reading time and achieve the same level of diagnostic accuracy as standard 1 mm T1ce images for the detection of brain metastases.

Methods

44 Patients were included in this retrospective study. Axial reformations of T1ce MP-RAGE (TR/TE=2300/2.25ms, resolution=1 mm^3) images were analysed and post-processed into 5 mm and 10 mm MIPs. Two readers evaluated the randomly assorted images and recorded reading time. Reading time differences were analysed using the Wilcoxon test, inter-reader statistics were performed using Bland-Altman plots.

Results

22.5 ± 61.2 seconds/study and 43.8 ± 159.9 seconds/study were saved using 5 mm and 10 mm MIPs respectively. Combined average sensitivity was 92.0% for 5 mm MIPs and 86.3% for 10 mm MIPs compared to standard 1 mm axial slices, with an average rate of 0.98 and 0.57 false positives per study, respectively.

Conclusion

While 5 mm and 10 mm T1ce MP-RAGE MIPs showed a clinical benefit in reducing reading times for evaluation of brain metastases, they should be used in conjunction with standard 1mm images for best sensitivity and specificity, a practice which possibly annuls their benefit.

1.1 Introduction

Brain metastases are the most common form of intracranial tumor in the adult population and despite earlier cancer detection and decreasing cancer mortality, the incidence of brain metastases appears to be increasing [1]. MRI is the most sensitive imaging modality for detecting brain metastases [2], outperforming CT [3] and is routinely used in staging and assessing treatment response. Just as important as detecting lesions, however, is assessing the number of brain metastases, which greatly influences therapy options. Advancements in cross-sectional imaging lead to a treatment shift from whole-brain radiation therapy (WBRT) alone to surgical resection of single brain metastases combined with WBRT, resulting in a survival benefit and better quality of life [4–6]. Furthermore, stereotactic radiosurgery (SRS) is employed in cases of surgically inaccessible lesions or as an alternative to surgery [7,8] yet the focussed nature of both SRS and microsurgical resection of metastases renders these therapies susceptible to treatment failure in cases where the entire burden of metastasis is not visualized. To ensure that patients receive optimal therapy, exact lesion characterization on MRI is imperative.

To visualize and assess brain lesions, radiologists face an ever-increasing pressure to perform faster and more efficiently- the current allotted time of 3 seconds per image [9] will only decrease as demands for radiological imaging increase [10]. One method to ensure that smaller lesions are not overlooked due to time constraints or visual/tedious fatigue is to increase their conspicuity. Delayed postcontrast imaging has been shown to visualize more metastases (one new lesion in 35.3% of cases) and greater volumes of metastases (25.4% mean increase in metastasis volume at 10 mins, additional 9% at 15 mins) [11], yet authors noted difficulty in differentiating true

tumor enhancement from leakage of contrast into the edematous areas surrounding the lesions. Another approach aiding radiologists is automated lesion detection; while early impacts of artificial intelligence in the detection of brain metastases seem promising [12], the only FDA approved AI-based software in neuroradiology to date has been limited to stroke imaging [13].

The usage of maximum intensity projections (MIPs) of contrast enhanced T1 weighed images (T1ce) for the detection of brain metastases proposes to increase reading efficiency by increasing lesion conspicuity while reducing in the number of images to be reviewed; MIPs have already been shown to increase sensitivity and decrease reading time in the detection of pulmonary nodules on CT [14,15]. MP-RAGE (and its equivalents among vendors SPGR/BRAVO, TFE, 3D Fast FE) is a well-established, widely used T1 weighted, gradient-echo pulse sequence [16] known for precise anatomical detail and high contrast between grey and white matter [17]; it has thus been consensus-recommended for brain tumor imaging[18]. One study evaluating detection of brain metastases reported a higher sensitivity using MIPs of SPGR (MP-RAGE equivalent) compared to source images- this study did not assess reading time or false positives [19]. Further studies on brain metastases report time savings, high sensitivities and low false positive rates using MIPs of black-blood sequences[20,21]; these sequences, however, aren't available on all MR systems [18]. The purpose of this work is to assess the clinical utility of MIPs through reading efficiency in time per exam and sensitivity/specificity in detecting brain metastases compared to T1ce MP-RAGE MRI source images. The standard 1 mm T1ce images serve as the reference standard.

1.2 Materials and Methods

1.2.1 Patients

This retrospective study was approved by the institutional review board. 50 MRI studies (average age 60, range 31-79) were included: 46 with brain metastases (origin: 23 pulmonary, 12 breast, 6 melanoma, 2 ovary, 3 other (cancer of unknown primary and sarcomas)) and 4 without brain metastases. Patients with leptomeningeal disease were not included in the study. Of the patients with brain metastases, 3 had a history of operative resection of metastases. Six studies were excluded due to motion artefacts.

1.2.2 MRI

Patients were scanned at our institution (University Hospital of Basel) on 3T and 1.5T magnetic resonance imaging (MRI) systems (Siemens Healthcare, Erlangen, Germany; 3T: Skyra, Verio, Prisma, 1.5T: Avanto, Espree) from December 2013 to August 2015. Axial reformations of original native and contrast enhanced T1 weighted (T1 and T1ce) magnetization-prepared rapid gradient-echo (MP-RAGE, acquired sagitally) images were utilized for analysis and post-processing into maximum intensity projections (MIP). Dotarem 0.2 mL/kg (0.1 mmol/kg) body weight was administered to all patients. Sequence parameters were identical for native and contrast enhanced T1w MP-RAGE sequences: TR/TE 3T Skyra 2300/2.3ms; 3T Verio 2000/3.3ms; 3T Prisma 1570/2.5ms; 1.5T Avanto 2700/5.0ms; 1.5T Espree 2700/5.0ms; FOV 256 x 256 mm, matrix size 256 x 256 mm; slice thickness 1 mm. Post-processing into axial 5 mm (4mm overlap) and 10 mm (9mm overlap) maximum intensity projections (MIP) was performed using a TeraRecon 3D workstation

(Aquarius iNtuition Viewer, Aquarius, TeraRecon, San Matteo, CA, USA). All MIPs were stored anonymously in the General Electric Centricity picture archiving and communication system (GE-PACS, General electric).

1.2.3 Image Analysis

Before analysis, all imaging data were anonymized. Two readers (CF and NH) with 11 and 5 years of experience in neuroradiology evaluated axial planes of the randomly assorted studies (1 mm source images, 5 mm MIPs and 10 mm MIPs) individually in sessions of 15 studies/day with a minimum of two weeks between sessions. Readers were blinded to MIP thickness and other image thicknesses were not available for comparison to the study currently being evaluated. Readers recorded reading time using stopwatches. As the 1 mm slices represented the current gold standard, differences in lesion numbers on 1 mm slices between readers were agreed upon in consensus in a second reading session. Metastases were defined as all discrete punctate or ring-enhancing lesions within the brain parenchyma.

1.2.4 Statistical Analysis

Reading times between the 1 mm slices and the 5 mm and 10 mm MIPs were compared using the non-parametric Wilcoxon test. Interreader correlation for the 5 mm and 10 mm MIPs was performed using Bland-Altman plots with regression analysis of the plots. Sensitivity of the differing methods was calculated after false negatives were established on 5 mm MIPs and 10 mm MIPs using the 1 mm slices as the gold standard. False positives were also established and were presented as a rate per study for 5 mm and 10 mm MIPs.

1.3 Results

Over 44 studies read, both the 5 mm and 10 mm MIPs resulted in time saved for both readers (Table 1: Reader 1, 5 mm MIP, 10 minutes 28 seconds saved in total, 10 mm MIP, 20 minutes 17 seconds saved in total; Reader 2, 5 mm MIP, 22 minutes 32 seconds saved in total, 10 mm MIP, 43 minutes 53 seconds saved in total). Thus, the combined average for time saved per study was 22.5 ± 61.2 seconds ($p = 0.0001$) for 5 mm MIPs and 43.8 ± 159.9 seconds ($p = 0.006$) for 10 mm MIPs. The reduction in reading time was significant using both 5 mm and 10 mm MIPs.

Lesion totals for both readers were as follows (Table 2):

1 mm, consensus 293 lesions; 5 mm MIPs: Reader 1, 294 lesions with 34 false positives and 33 false negatives, Reader 2: 327 lesions with 52 false positives and 18 false negatives; 10 mm MIPs: Reader 1, 256 lesions with 21 false positives and 58 false negatives, Reader 2: 286 lesions with 29 false positives and 36 false negatives.

Average number of lesions/study was: 1 mm, 6.7, 5 mm MIPs,7.1, 10 mm MIPs, 6.2.

Metastasis size distribution is as follows: 1 mm to 4 mm 140/293 (48%), 5 mm to 8 mm 87/293 (30%), 9 mm to 12 mm 33/293 (11%), 13 mm to 16 mm 15/293 (5%), 17 mm to 19 mm 9/293 (3%), ≥20 mm 9/293 (3%).

This resulted in a combined average sensitivity of 92.0% for 5 mm MIPs and 86.3% for 10 mm MIPs and an average rate of 0.98 and 0.57 false positives per study, respectively.

Inter-reader statistics were calculated using Bland-Altman plots (Figure 1). For 5 mm MIPs, regression analysis revealed no systematic differences between the two readers ($t= 0.602$, $sig= 0.551$). For 10 mm MIPs, regression analysis revealed a systematic difference ($t= 2.311$, $sig= 0.026$) which can be attributed to the different thresholds

individual readers had in deciding if a lesion was present or not: Reader 2 accumulated a higher total lesion score (286 vs 256) and recorded more false positives (29 vs 21) but less false negatives (36 vs 58).

1.4 Discussion

In this study, we could show that the use of maximum intensity projections of T1ce MP-RAGE MRI source images alone for the evaluation of brain metastasis resulted in decreased reading times which was statistically significant, however lead to a higher number of false positives and false negatives when compared to 1mm slices. This was especially pronounced in the thickest MIPs used in this study (10 mm).

Reasons for decreased sensitivity of metastases on MIPs were the thickened appearance of (enhancing) dural structures such as the tentorium and the dura of the convexities (Figure 2), especially near the vertex- this effect was noted especially for the smaller lesions. Furthermore, the superimposition of normally enhancing structures such as the pineal gland, the pituitary gland / cavernous sinus, and the choroid plexus essentially obscured visualization of metastases located either superiorly or inferiorly to these areas. In many instances where (generally bigger) multiple metastases were found to overlap on axial slices, it could not be determined on MIPs if they were two separate lesions or a multilobular single lesion. These effects were more pronounced on 10 mm MIPs compared to 5 mm MIP resulting in a lower sensitivity for 10 mm MIPs.

Specificity was influenced by factors similar to those affecting sensitivity. First, focal enhancing vascular structures of the skull, such as hemangiomas, or structures along the dura (Figure 3) were superimposed onto the brain parenchyma near the vertex and basal aspects of the skull, creating the illusion of a focal enhancing parenchymal lesion. The averaging effect of the MIPs on the parenchyma obscured any darker (hypointense) parenchymal lesions such as cystic lesions or resection cavities - therefore, multiple enhancing lesions along the border of the cystic lesion were not

seen as associated to one cystic lesion and recorded as separate. In these cases, the 1 mm slices must be referred to. Due to this, the 1 mm slices should, in fact, be consulted for every study, negating the benefit of time saving from the MIPs. Interestingly, less false positives were found on 10 mm MIPs (rate 0.57 false positives per study) than on 5 mm MIPs (rate of 0.98 false positives per study) possibly due to effects also decreasing sensitivity.

Previous studies on comparing MIPs to source images for detection of metastases on brain MRI report heterogeneous results. Sepulveda et al. report increased detection of metastases on MIPs of contrast-enhanced, T1-weighted SPGR images (equivalent to MPRAGE) compared to source images[19]. While this study did not assess false positives, they suggested that source images were better for detecting metastases closer to enhancing brain structures such as the choroid plexus. Bae et al. report a higher detectability of brain metastases and lower false positive rates using source images and MIPs of a black blood sequence (iMSDE-TSE) compared to source images and MIPs of a non-black-blood sequence (3D-GRE)[20]. Both of these studies, however, suggest MIPs be used together with source images for best diagnostic performance, effectively nullifying potential time savings. A recent study by Yoon et al. is the first to suggest that MIPs of another sequence with black-blood properties (CUBE) could replace source images altogether [21]. They admit, however, that faulty black-blood suppression of short-segment vascular structures and superimposition-effects of patients with innumerable metastases represent obstacles to full replacement of source images.

Limitations of the present study are: For potential sources of error, the nature of the 1 mm axial slices compared to the 5 mm and 10 mm MIPs allowed readers to

comprehend which image they were reading and were resultingly not fully blinded- this is a systematic limitation in all previously published studies comparing MIPs to source images. Although we didn't exclude postoperative studies in the cohort, the artefacts, especially dural thickening, is another potential source of error. We felt, however, that including postoperative MRIs was more representative of clinical routine and in fact a strength of our study. Finally, no histologic data was available for determination of ground truth for metastases as surgical resection of multiple metastases is usually not performed.

In this study, we could show that the use of maximum intensity projections of axial T1ce MP-RAGE MRI source images alone for the detection of brain metastasis detection resulted in a statistically significant decrease in reading time, however led to a higher number of false positive and false negative results.

1.5 Conclusion

While 5 mm and 10 mm T1ce MP-RAGE MIPs showed a clinical benefit in reducing reading times for evaluation of brain metastases, they should be used in conjunction with standard 1mm images for best sensitivity and specificity, a practice which possibly annuls their benefit.

Conflict of interest

The Author declares that there is no conflict of interest.

Data availability statement

The data that support the findings of this study are available from the corresponding author upon reasonable request.

Ethics Statement

This retrospective study was approved by the institutional review board. Because of the retrospective nature of the study, informed consent was waived.

References

[1] Gavrilovic IT, Posner JB. Brain metastases: epidemiology and pathophysiology. J Neurooncol 2005;75:5–14. https://doi.org/10.1007/s11060-004-8093-6.

[2] Fink KR, Fink JR. Imaging of brain metastases. Surg Neurol Int 2013;4:S209-219. https://doi.org/10.4103/2152-7806.111298.

[3] Schellinger PD, Meinck HM, Thron A. Diagnostic accuracy of MRI compared to CCT in patients with brain metastases. J Neurooncol 1999;44:275–81.

[4] Hatiboglu MA, Wildrick DM, Sawaya R. The role of surgical resection in patients with brain metastases. Ecancermedicalscience 2013;7. https://doi.org/10.3332/ecancer.2013.308.

[5] Patchell RA, Tibbs PA, Walsh JW, Dempsey RJ, Maruyama Y, Kryscio RJ, et al. A randomized trial of surgery in the treatment of single metastases to the brain. N Engl J Med 1990;322:494–500. https://doi.org/10.1056/NEJM199002223220802.

[6] Vecht CJ, Haaxma-Reiche H, Noordijk EM, Padberg GW, Voormolen JH, Hoekstra FH, et al. Treatment of single brain metastasis: radiotherapy alone or combined with neurosurgery? Ann Neurol 1993;33:583–90. https://doi.org/10.1002/ana.410330605.

[7] Baumert BG, Rutten I, Dehing-Oberije C, Twijnstra A, Dirx MJM, Debougnoux-Huppertz RMTL, et al. A pathology-based substrate for target definition in radiosurgery of brain metastases. Int J Radiat Oncol Biol Phys 2006;66:187–94. https://doi.org/10.1016/j.ijrobp.2006.03.050.

[8] Chang EL, Wefel JS, Hess KR, Allen PK, Lang FF, Kornguth DG, et al. Neurocognition in patients with brain metastases treated with radiosurgery or radiosurgery plus whole-brain irradiation: a randomised controlled trial. Lancet Oncol 2009;10:1037–44. https://doi.org/10.1016/S1470-2045(09)70263-3.

[9] McDonald RJ, Schwartz KM, Eckel LJ, Diehn FE, Hunt CH, Bartholmai BJ, et al. The effects of changes in utilization and technological advancements of cross-sectional imaging on radiologist workload. Acad Radiol 2015;22:1191–8. https://doi.org/10.1016/j.acra.2015.05.007.

[10] Diagnostic/Medical Imaging Market Size & Share | Industry Report, 2025 n.d. https://www.grandviewresearch.com/industry-analysis/medical-imaging-systems-market (accessed April 3, 2018).

[11] Kushnirsky M, Nguyen V, Katz JS, Steinklein J, Rosen L, Warshall C, et al. Time-delayed contrast-enhanced MRI improves detection of brain metastases and apparent treatment volumes. J Neurosurg 2016;124:489–95. https://doi.org/10.3171/2015.2.JNS141993.

[12] Charron O, Lallement A, Jarnet D, Noblet V, Clavier J-B, Meyer P. Automatic detection and segmentation of brain metastases on multimodal MR images with a deep convolutional neural network. Comput Biol Med 2018;95:43–54. https://doi.org/10.1016/j.compbiomed.2018.02.004.

[13] Commissioner O of the. Press Announcements - FDA permits marketing of clinical decision support software for alerting providers of a potential stroke in patients n.d. https://www.fda.gov/NewsEvents/Newsroom/PressAnnouncements/ucm596575.htm (accessed April 3, 2018).

[14] Valencia R, Denecke T, Lehmkuhl L, Fischbach F, Felix R, Knollmann F. Value of axial and coronal maximum intensity projection (MIP) images in the detection of pulmonary nodules by multislice spiral CT: comparison with axial 1-mm and 5-mm slices. Eur Radiol 2006;16:325–32. https://doi.org/10.1007/s00330-005-2871-1.

[15] Jankowski A, Martinelli T, Timsit JF, Brambilla C, Thony F, Coulomb M, et al. Pulmonary nodule detection on MDCT images: evaluation of diagnostic performance using thin axial images, maximum intensity projections, and computer-assisted detection. Eur Radiol 2007;17:3148–56. https://doi.org/10.1007/s00330-007-0727-6.

[16] Mugler JP, Brookeman JR. Three-dimensional magnetization-prepared rapid gradient-echo imaging (3D MP RAGE). Magn Reson Med 1990;15:152–7.

[17] Deichmann R, Good CD, Josephs O, Ashburner J, Turner R. Optimization of 3-D MP-RAGE sequences for structural brain imaging. NeuroImage 2000;12:112–27. https://doi.org/10.1006/nimg.2000.0601.

[18] Ellingson BM, Bendszus M, Boxerman J, Barboriak D, Erickson BJ, Smits M, et al. Consensus recommendations for a standardized Brain Tumor Imaging Protocol in clinical trials. Neuro-Oncol 2015;17:1188–98. https://doi.org/10.1093/neuonc/nov095.
[19] Sepulveda F, Yáñez P, Carnevale MD, Romero C, Castillo M. MIP Improves Detection of Brain Metastases. J Comput Assist Tomogr 2016;40:997–1000. https://doi.org/10.1097/RCT.0000000000000466.
[20] Bae YJ, Choi BS, Lee KM, Yoon YH, Sunwoo L, Jung C, et al. Efficacy of Maximum Intensity Projection of Contrast-Enhanced 3D Turbo-Spin Echo Imaging with Improved Motion-Sensitized Driven-Equilibrium Preparation in the Detection of Brain Metastases. Korean J Radiol 2017;18:699–709. https://doi.org/10.3348/kjr.2017.18.4.699.
[21] Yoon BC, Saad AF, Rezaii P, Wintermark M, Zaharchuk G, Iv M. Evaluation of Thick-Slab Overlapping MIP Images of Contrast-Enhanced 3D T1-Weighted CUBE for Detection of Intracranial Metastases: A Pilot Study for Comparison of Lesion Detection, Interpretation Time, and Sensitivity with Nonoverlapping CUBE MIP, CUBE, and Inversion-Recovery-Prepared Fast-Spoiled Gradient Recalled Brain Volume. AJNR Am J Neuroradiol 2018. https://doi.org/10.3174/ajnr.A5747.

Tables

	5 mm MIP	10 mm MIP
Reader 1	14.3 ± 63.4 s	27.7 ± 112.2 s
Reader 2	30.7 ± 58.4 s	59.8 ± 207.6 s
Combined Average	22.5 ± 61.2 s	43.8 ± 159.9 s

Table 1 Time savings in seconds/study with standard deviation for 5 mm MIPs and 10 mm MIPs compared to 1 mm source images

	Reader 1	Reader 2	Combined Average/Study
		1 mm	
Total Lesions	293	293	6.7
		5 mm	
Total Lesions	294	327	7.1
False Positives	34	52	0.98
False Negatives	33	18	Sensitivity 92.0%
		10 mm	
Total Lesions	256	286	6.2
False Positives	21	29	0.57
False Negatives	58	36	Sensitivity 86.3%

Table 2: Total Lesions on 1 mm, 5 mm, and 10 mm images for both readers and number of false positives and false negatives.

Figure 1

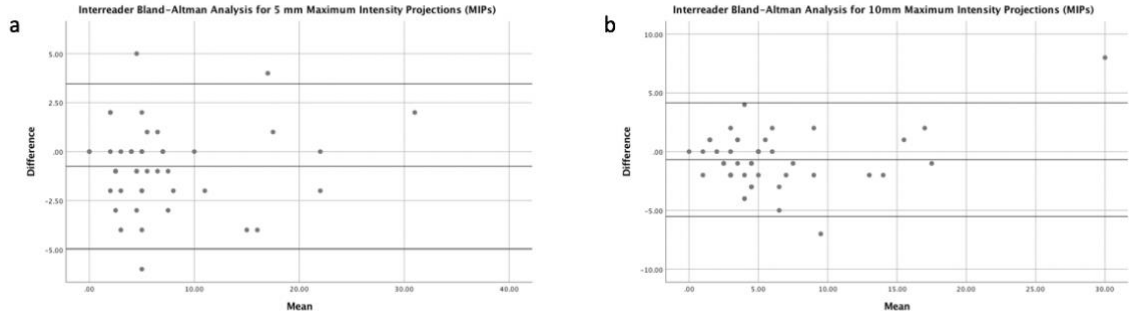

Figure 1 Interreader Bland-Altman Analysis for 5 mm MIPs (left) and 10 mm MIPs (right).

Figure 2

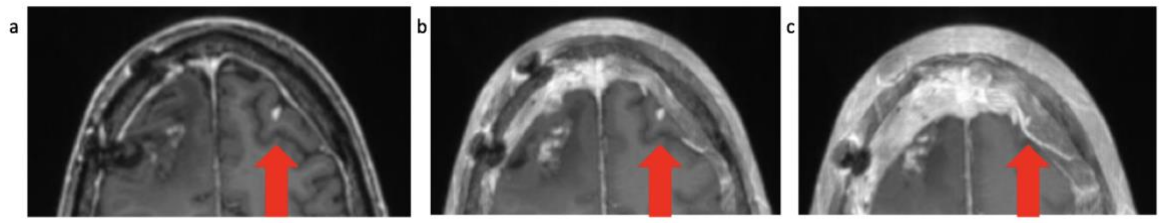

Figure 2 Example of the three data sets: left 1 mm images, middle 5 mm MIPs, and right 10 mm MIPs. An ovoid lesion of the left middle frontal gyrus is clearly depicted on 1 mm images, at the border of the overlapping dura on 5 mm MIPs, and obscured on 10 mm MIPs

Figure 3

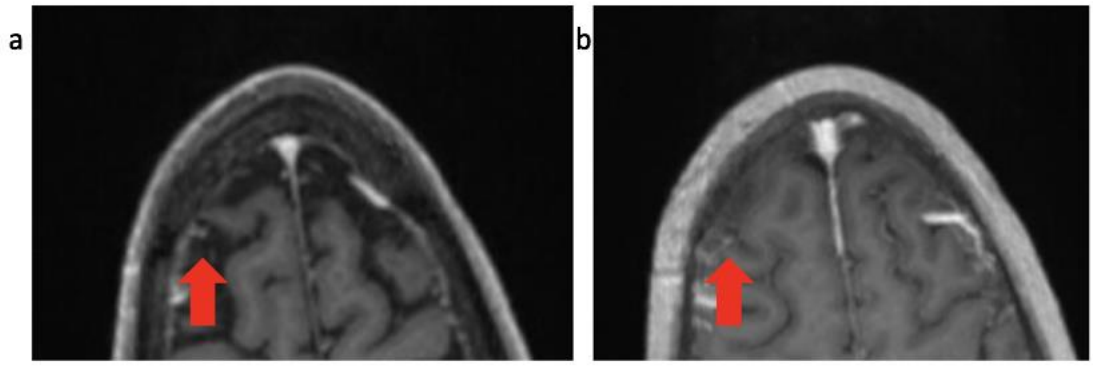

Figure 3 Example of a false positive lesion (right: 1 mm slices, left: 5 mm MIP): a seemingly punctate enhancing lesion is seen on the cortex of the right middle frontal gyrus on 5 mm MIPs (right). After correlation to the 1 mm images (left), this structure is revealed to be a focal irregularity of the dura projecting into the subarachnoid space, most likely representing a vascular structure.